



Protective Mechanism of MIF Inhibitor ISO-1 on Intrahepatic Bile Duct Cells in Rats with Severe Acute Pancreatitis

Bin Wang¹ · Kailiang Zhao¹ · Wenjuan Hu² · Youming Ding¹ · Weixing Wang¹

Received: 19 February 2020 / Accepted: 10 October 2020 / Published online: 29 October 2020
© Springer Science+Business Media, LLC, part of Springer Nature 2020

Abstract

Aims This study aimed to explore the protection mechanism of ISO-1 on severe acute pancreatitis-associated intrahepatic bile duct (IBD) injury in rats.

Methods Forty-eight specific-pathogen-free male Wistar rats were randomly divided into four groups ($N=12$): a sham operation group (SO group), a severe acute pancreatitis model group (SAP group), a ISO-1 treatment group (ISO-1 + SAP group), and a ISO-1 control group (ISO-1 + SO group). All rats were killed after 12 h of being made models. Immunohistochemistry was used to detect the expression of MIF and P38 in IBD cells. MIF mRNA expression in IBD cells was observed using real-time fluorescent quantitative polymerase chain reaction (real-time PCR). In addition, Western blotting was performed to detect the protein expression of P38, phosphorylated P38 (P-P38), nuclear factor- κ B (NF- κ B p65), and tumor necrosis factor alpha (TNF- α). Enzyme-linked immunosorbent assays were used to analyze the levels of TNF- α , IL-1 β , and IL-6 in the IBD of rats.

Results Compared with SAP, after treatment with ISO-1, the pathological injuries of pancreas, liver, and IBD cells in ISO-1 treatment group remarkably relieved. The expression of MIF in the IBD cells was significantly downregulated both at mRNA and at protein levels in ISO-1 treatment group. Besides, the protein expression levels of P38, P-P38, NF- κ Bp65, TNF- α , IL-1 β , and IL-6 in the IBD in rats were also significantly decreased in ISO-1 treatment group (all $P < 0.05$).

Conclusion ISO-1 may protect the IBD cells, reduce pathological injuries, and reduce the inflammatory response in SAP rats. Its mechanisms may be via inhibiting the expression of MIF and then blocking the activation of p38-MAPK and NF- κ B signaling pathway.

Keywords Macrophage migration inhibitory factor inhibitor · Severe acute pancreatitis · Intrahepatic bile duct cell · P38 · Cytoprotection

Abbreviations

MIF	Macrophage migration inhibitory factor
ISO-1	A specific small molecule inhibitor of MIF
SAP	Severe acute pancreatitis
AP	Acute pancreatitis
IBD	Intrahepatic bile duct
SPF	Specific-pathogen-free
SO	Sham operation

NF- κ B	Nuclear factor- κ B
TNF	Tumor necrosis factor
ELISA	Enzyme-linked immunosorbent assays
IL	Interleukin
MODS	Multiple organ dysfunction syndrome
MOF	Multiple organ failure
SIRS	Systemic inflammatory response syndrome
ARDS	Acute respiratory distress syndrome
AP	Acute pancreatitis
MAPK	Mitogen-activated protein kinase
ICAM	Intercellular adhesion molecule
VCAM	Vascular cell adhesion protein
MCP	Monocyte chemoattractant protein
HRP	Horseradish peroxidase
H&E	Hematoxylin and eosin
PBS	Phosphate-buffered saline

✉ Bin Wang
wb7112@126.com

¹ Hubei Key Laboratory of Digestive System Disease, Department of Hepatobiliary Surgery, Renminbi Hospital of Wuhan University, Wuhan 430060, Hubei Province, China

² Department of Anesthesiology, Renmin Hospital of Wuhan University, Wuhan 430060, Hubei Province, China

IOD Integral optical density
SEM Standard error of the mean

Introduction

Due to its fast onset and rapid progress, the dangerous condition SAP (severe acute pancreatitis) accompanied by MODS (multiple organ dysfunction syndrome) often leads to high mortality and seriously threatens human health. Currently, due to the lack of specific clinical treatment for SAP, there are no effective preventative methods for it in combination with MODS. According to our previous study, macrophage migration inhibitory factor (MIF), as an important proinflammatory factor, amplifies the inflammatory response of intrahepatic bile duct (IBD) cells in SAP by activating the p38-MAPK signaling pathway, which aggravates injury to IBD cells [1].

Studies have shown that the phosphorylation level of p38-MAPK is significantly reduced in a MIF gene knockout macrophage model. In addition, the lack of endogenous MIF in macrophages increases the sensitivity of macrophages to glucocorticoids and leads to a reduction in inflammatory cytokines in downstream cells, including TNF- α cells and NF- κ B cells [2]. Studies by Chia-Chang Chuang et al. [3] suggested that the application of the MIF inhibitor ISO-1 could significantly reduce the generation and release of inflammatory factors such as IL-6, IL-8, and TNF- α during the inflammatory reaction by regulating the activity of the p38-MAPK signaling pathway and NF- κ B, significantly stimulating inflammatory injury. A study on lung injury by Takahashi et al. [4] found that MIF enables neutrophils, macrophages, and some other inflammatory cells to aggregate in the alveolar cavity by activating the ERK1/2 MAPK pathway. The MIF inhibitor ISO-1 can effectively inhibit MIF-induced ERK1/2 MAPK phosphorylation, thereby inhibiting the release of chemokines downstream of the pathway and reducing the aggregation of neutrophils.

Therefore, if the activity of MIF can be blocked in SAP, the corresponding inflammatory response can be inhibited, and then, the damage to organ function can be reduced, which may provide new methods and strategies for the treatment of multiple organ injuries related to SAP [3, 5].

According to our earlier study, there was obvious pathological damage in the hepatic bile duct cells of SAP rats and MIF expression in hepatic bile duct cells was enhanced, which promoted inflammatory injury by activating the p38-MAPK signaling pathway.

ISO-1 ((S,R)-3-(4-hydroxyphenyl)-4,5-dihydro-5-isoxazole methyl ester) is a specific small molecule inhibitor of MIF, a dopa-chromium isomerase inhibitor derivative that is also a tautomerism enzyme inhibitor. ISO-1 can inhibit MIF isomerase and its biological activities by inhibiting

MIF binding to the membrane receptor CD74. Moreover, ISO-1 has no obvious effects on other inflammatory cells or immune functions [5]. It has been successfully applied to basic research in animal models to interfere with a variety of diseases, such as ulcerative colitis, multiple organ dysfunction due to endotoxaemia, inflammatory diseases, and ischemia–reperfusion injury. Based on the discoveries above, determining whether the MIF inhibitor ISO-1 could relieve IBD cell injury through inhibition of p38-MAPK activation and lead to the downregulation of downstream inflammation-related factors is promising for SAP treatment.

In this study, a rat SAP model was constructed, and ISO-1 was applied as a specific MIF inhibitor to observe its protective effects on IBD cells. We believe our discovery may provide some experimental evidence leading to a new targeted SAP therapeutic treatment.

Materials and Methods

Experimental Animal Groups

Forty-eight specific-pathogen-free (SPF) male Wistar rats weighing 200 g to 250 g were purchased from Huafukang Biological Technology Co., Ltd. (Beijing). The experimental animal quality qualified card number was 11401300010796. The rats were randomly divided into four groups ($N = 12$ each): the SO (sham operation) group, SAP group, ISO-1 treatment group (ISO +SAP), and ISO-1 drug control group (ISO-1 + SO). The housing conditions were as follows: 22 °C \pm 2 °C, 55% \pm 5% humidity, artificial lighting for 12 h per day, and free access to food and water. All rats were fasted for 12 h before the experiment but were allowed water. All animal experiments in this study were reviewed and approved by the Ethics Committee of Renmin Hospital of Wuhan University.

Main Reagents

The primary antibody p38 was purchased from Guge Biological Technology Co., Ltd. (Wuhan). The secondary antibody (goat anti-rat) and the primary antibody (rabbit anti-P38 polyclonal antibody) were purchased from DAKO, Denmark. A Reverse Aid First-Strand cDNA short kit was purchased from Thermo Fisher (USA), quantitative fluorescence PCR kits were purchased from FastStart, and Universal SYBR Green Master (Rox) was obtained from Roche (USA). The PCR primers were synthesized by Invitrogen Biotechnology Co., Ltd. (China). ELISA kits for TNF- α , IL-1 β , and IL-6 were purchased from Xinbosheng Biotechnology Co., Ltd. (Shenzhen), and the bicinchoninic acid (BCA) protein quantitative detection kit was obtained from Bio-Rad (USA). Actin and NF- κ B p65 antibodies for Western blotting were

purchased from Santa Cruz (USA), and P38 and p-p38 antibodies were acquired from CST (USA). The TNF- α antibody was obtained from Abcam (UK), and the horseradish peroxidase (HRP)-labeled polyclonal antibody was purchased from KPL (USA). ISO-1 was purchased from Sigma (USA), dissolved in DMSO at a concentration of 1.6 mg/ml, and was applied at the dose of 0.2 ml/100 g according to the weight of each rat.

Experimental Methods and Test Targets

Animal Model Preparation

Rats in the SAP group were anaesthetized with isoflurane (induced with 5% isoflurane and maintained with 3% in 2 l/min oxygen flow in a sealed container). The pancreaticobiliary ducts of the SAP group rats were injected with a 5% solution of taurocholic acid sodium at a constant rate of 0.1 ml/min using a micropump (dosage: 0.1 ml/100 g body weight), and the SO group was injected with the same volume of saline solution. For the ISO-1 treatment group (SAP + ISO-1 group), the MIF inhibitor ISO-1 (1.6 mg/ml, dissolved in 5% DMSO solution) was intraperitoneally injected into rats 30 min before SAP modeling. In the ISO-1 drug control group (SO + ISO-1 group), the sham operation model was prepared by intraperitoneal injection of ISO-1 (1.6 mg/ml, dissolved in 5% DMSO solution) into the rats 30 min before surgery. Twelve hours was taken as the observation point. The incision was closed with a continuous 3-0 silk suture, and 20 mL/kg saline solution was injected subcutaneously into the back to compensate for the fluid loss associated with the surgical procedure. All animals recovered from surgery.

Sample Acquisition

Rats in each group were prepared by laparotomy 12 h after the operation. The method used for processing specimens was as follows. Rats were anaesthetized with isoflurane (induced with 5% isoflurane and maintained with 3% in 2 l/min oxygen flow in a sealed container). A blood specimen was collected through inferior vena cava puncture, and then, serum was collected by centrifugation for 10 min at 2000 rpm. All of the pancreatic and hilar bile duct tissues and 1.0 cm³ of the left lobe of the liver were resected. The adipose tissues surrounding the pancreas were removed. The pancreatic head was fixed in 4% paraformaldehyde solution, embedded in paraffin, and sectioned. Sections were stained by hematoxylin and eosin (H&E). Finally, the pathological changes of the tissues were assessed. The remaining pancreas samples were stored in cryopreservation tubes in liquid nitrogen. The hepatic bile duct tissues were divided into

3 parts. Part 1 was fixed in 4% formaldehyde diluted with PBS for conventional paraffin sectioning. Part 2 was kept frozen in liquid nitrogen for later use. Part 3 was prepared in precooled 2.5% glutaraldehyde for electron microscopy. The other specimens were stored at -80°C . After collecting the specimens, the experimental rats were sacrificed by spinal dislocation.

Separation and Purification Methods for IBD Cells

Hilar bile duct tissues were placed into a centrifuge tube (volume: 10 ml), and 2 ml of 90% Percoll was added. Then, 2 ml of 32% Percoll solution was added slowly into the 90% Percoll solution. The dispersed liver cells were filtered using a 200-mesh nylon filter, and then, the filter was oscillated at 37°C to separate the white IBD tissues. Subsequently, the cells were placed into a solution of digestive juices containing 0.25% trypsin and 0.05% type IV collagenase, oscillated for 50 min at 37°C , and then centrifuged at 300 g. The pellet was resuspended, and the cell suspension was rich in IBD cells.

H&E Staining

The pancreas, liver, and IBD tissues obtained from the experimental rats were routinely embedded in paraffin and sectioned. The section thickness was set to 4 μm . Sections were stained by H&E via the following steps. Fresh tissue sections were placed into xylene and soaked and dewaxed for 5–10 min. Then, the tissue was transferred into a solution of xylene and 100% alcohol (V/V = 1:1) for 5 min before being rehydrated in a graded series of ethanol: 95%, 85%, and 70%. The sections were placed in each alcohol concentration for 3–5 min and then washed with distilled water for 2 min. The sections were then stained by hematoxylin for 10–15 min and eosin for 2–5 min. Finally, the sections were dehydrated in alcohol, made transparent using xylene, and sealed with neutral gum.

Pathological Inspection of Pancreatic Tissues

H&E-stained pancreas sections were observed under a light microscope, and pathology scores were assessed based on the Schmidt J standard [6] using the following four aspects: pancreatic edema, necrosis degree of the pancreatic acini and gland duct, hemorrhage of the gland and fat liquefaction necrosis, and inflammation and blood vessel inflammatory infiltrates.

Liver and IBD Cell Pathological Inspection

Liver and IBD cell pathological injury was judged by Suzuki's grade standards [7]. In each case, four different

sections and five randomly chosen areas were selected, magnified 200 \times , and scored using the counting method. Level 0 was equal to little or no damage observed, whereas level 1 injury included mild damage, such as cytoplasmic vacuoles and focal nuclear pyknosis (score: 1 point). Level 2 consisted of moderate to severe damage, such as wide-ranging nuclear pyknosis and absent cell borders (score: 2 points). Finally, level 3 showed serious necrosis, including hepatic cord disintegration, bleeding, and neutrophil infiltration (score: 3 points).

Ultrastructural Alteration of IBD Cells in Rats

The ultrastructural changes of rat IBD cells were observed by electron microscopy. The ultrathin tissue slice preparation methods for IBD tissues were as follows. At 4 °C, 1-mm³ IBD tissue pieces were fixed in 2% glutaraldehyde sodium phosphate buffer for approximately 60 min, followed by washing in 0.1 mol/L phosphate buffer overnight, and then, the IBD tissue mass was washed with osmium tetroxide phosphate buffer solution for 90 min. The IBD tissue blocks were then dipped into pure acetone following resin embedding and baked in porous rubber embedding plates. The ultrathin sections were stained with 2% uranium acetate and 6% lead citrate for 30 min each. The prepared IBD tissue sections were placed under a Hitachi H-300 transmission electron microscope for imaging.

Immunohistochemical Method for the Determination of MIF and P38 Expression Levels in IBD Cells

The MIF and P38 expression levels in IBD cells were determined by immunohistochemical methods according to the manufacturer's protocols (Dako, Denmark). The intensity of the immunohistochemical signal and the area of labeled IBD cells were measured. A tan reaction product represented positive expression of MIF and P38. Areas in the microscope field were randomly selected in each section, and photographs were taken at 200 \times magnification for each group. Each image was analyzed, and an integral optical density (IOD) value of positive expression was generated using Image-Pro Plus 6.0 software. Higher IOD values indicated stronger positive expression. The average IOD value of all of the images taken for each group was used as the IOD value for that group, and the values are presented as the mean \pm standard deviation (SD). Significant differences among various groups were analyzed with GraphPad Prism 5.01 software.

Contents of TNF- α , IL-6, and IL-1 β in IBD Cells

For ELISA, a suspension containing a suitable number of IBD cells was created. The standard well, blank well, and test sample well (including the main and deputy wells) were preset separately. According to the steps listed in the ELISA kit manual, 100 μ l of standard liquid was added into the standard well, and the same volume of test sample was pipetted into the test sample well. The plate was gently shaken and thermostatically incubated at 37 °C for 1 h. Then, 100 μ l of biotin-labeled antibody working solution was pipetted into each well followed by thermostatic incubation under the same conditions. Following the removal of the liquid in the wells and drying, 100 μ l of HRP-labeled streptavidin working solution was added to each well and then incubated. Next, 90 μ l of the substrate reaction solution was added to each well, and the color reaction was allowed to develop at 37 °C for 15–30 min in the dark. Then, 50 μ l of end solution was added to each well to terminate the reaction. The optical density (OD) of every well was measured at 450 nm. A standard curve was generated, and levels of TNF- α , IL-1 β , and IL-6 in IBD cells were calculated using the OD values.

Real-Time PCR for MIF and TNF- α mRNA Expression Levels in IBD Cells

First, 100 mg of IBD cell suspension was homogenized, and 250 μ l of trichloromethane was added. After allowing the mixture to rest for 3 min, it was centrifuged at 13,000 rpm for 8 min at 4 °C, and the supernatant was transferred to a new centrifuge tube. Then, isopropyl alcohol was added at 0.8 times the volume, and the mixture was held at –20 °C for 15 min before centrifugation for 10 min. Finally, the pellet was dried and resuspended. Next, 2 μ g of RNA solution and 1 μ l of reverse transcriptase were placed in the fluorescence quantitative PCR instrument to start the reverse transcription reaction. Once the reaction was complete, the products were heated to 80 °C for 5 min to inactivate the reverse transcriptase. Then, PCR amplification and quantitative analysis were performed. The cycle parameters were as follows: denaturation at 95 °C for 10 min, followed by 40 cycles at 95 °C for 15 s and 60 °C for 60 s. A solubility curve was run at 75–91 °C every 20 s. The cycle threshold (Ct) value was obtained by detecting the intensity of the fluorescent signal, which changed with PCR amplification, in real time. The $\Delta\Delta$ CT method was used to calculate the abundance value of the target gene. The PCR primers are listed in Table 1.

Table 1 The PCR primers of MIF mRNA and TNF- α mRNA

Primer information	Primer name	Primer sequences (5'–3')	Fragment length (bp)	Annealing temperature (°C)
NM_031144	R- β -actin-S	TGCTATGTTGCCCTAGAC	240	60
	R- β -actin-A	GTTGGCATAGAGGTCTTTACGG		60
NM_031051.1	R-Mif-S	GACTTTAGTGTGGCAGGAGCG	92	60
	R-Mif-A	GCTTGCTGTAGTTGCGGTTCT		60
NM_012675.3	R-TNF- α -S	CTTCTCATTCTGCTCGTGG	201	60
	R-TNF- α -A	TCCGCTTGGTGGTTGCTAC		60

Western Blotting to Determine the NF- κ Bp65, P38, P-P38, and TNF- α Protein Expression Levels in IBD Cells

First, 50 mg of the IBD cell suspension was mixed with protease inhibitors, and after a few minutes, 500 μ l of tissue protein extract was added. The mixture was homogenized for 5 min in an ice bath and centrifuged at 12,000 rpm for 30 min. The supernatant contained the proteins. Protein concentrations were determined by the Bradford method. Sodium dodecyl sulfate–polyacrylamide gel electrophoresis (SDS-PAGE) was performed, and based on the marker position and target protein molecular weight, the colloid was cut and labeled. Nitrocellulose (NC) membranes and filter papers were dipped in transfer buffer for 5 min and then run for 2 h at 200 mA. The NC membranes were sealed with membrane sealing fluid for 2 h after being rinsed thoroughly 5 times with Tris-buffered saline (TBS). Subsequently, the membrane was incubated with diluted primary antibody in fresh membrane sealing fluid overnight at 4 °C. A diluted secondary HRP-labeled antibody was incubated with the NC membranes at room temperature for 1 h. Then, the NC membranes were rinsed five times with TBS 10 \times (TBST) buffer with shaking. The membranes were transferred to chemiluminescence color liquid and incubated for 2 min. Then, the residual liquid was removed, and the NC membranes were wrapped and exposed in cassettes. Next, they were developed and fixed in the corresponding developing and fixing agents. Finally, the films were scanned and photographed. The experiments were repeated three times. The target protein OD value was analyzed using the Alpha software processing system.

Statistical Analysis

Data are presented as the mean \pm standard error of the mean (SEM) and were analyzed with GraphPad Prism 5.01 (GraphPad Software, Inc., USA). *T* tests were used to evaluate differences in the means between two samples, and single factor analysis of variance was used for multiple comparisons between multiple sample means. Results with *P* values < 0.05 were considered statistically significant.

Results

Pancreatic Pathological Injury

In the SO group and ISO-1 drug control group, the rats did not exhibit significant pathological injury to the pancreatic organizational structure that could be observed by the naked eye. In contrast, in the SAP group, changes in the pancreas could be observed 5 min post-injection: the pancreas became red, edemic, and hemorrhagic. After 12 h, congestion and swelling of the bowel, abundant ascites, a darker purple color, and extensive necrosis of the pancreas were apparent and saponification spots developed in the mesenteric and peritoneal organization. Twelve hours after initiation of the SAP animal model, large areas of pancreatic cells exhibited necrosis, and the pancreatic gland structure was mostly destroyed. In contrast, these pathological changes were obviously reduced in the ISO-1 treatment group compared with the SAP group. Statistically significant differences (*P* < 0.05) were observed between the SAP group and the ISO-1 treatment group (Figs. 1a–e, 4a–d).

Liver and IBD Pathological Injury

Liver cell injuries in the rats were observed by light microscopy in the SAP group. Dot degeneration and large areas of necrosis in liver cells were observed to exist at the same time, and some hepatic cords disintegrated. In the ISO-1 treatment group, necrosis of the hepatocytes was alleviated, and some hepatic cords were slightly disordered or showed only punctate degeneration and necrosis. The pathology score in the ISO-1 treatment group was lower than that in the SAP group. There were no significant injuries to liver cells in the other two groups, the SO group and the ISO-1 drug control group (Fig. 2a–e).

In the SAP group, IBD cells showed large areas of cell necrosis and a large number of infiltrating inflammatory cells. In the ISO-1 treatment group, IBD cells also showed necrosis, a disordered arrangement and inflammatory cell infiltration, but the degree of damage was significantly reduced compared with that in the SAP group. The pathological scores of IBD cell injuries in the SAP group

were significantly higher than those in the ISO-1 treatment group. There was a significant difference ($P < 0.05$) between the two groups (Fig. 3a–e). IBD cells did not

show specific damage in the other two groups, the SO group and the ISO-1 drug control group.

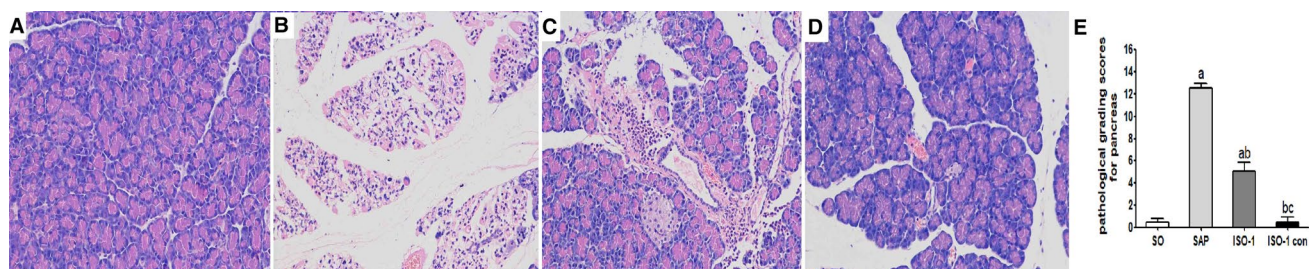


Fig. 1 Pathological changes in rat pancreatic tissue observed by H&E staining (magnification: 200×). **a** and **d** SO and ISO-1 con group: the pancreatic tissues and structure are clear and complete. **b** SAP group: The normal structure of the pancreas is destroyed, and the acinar structure disappears, and the acinar cells edema and necrosis are obvious, the leaf septum expanding extensively, inflammatory cell infiltration extensive, extra-vascular and intra-septal bleeding mas-

sive, and peripancreatic fat necrosis. **c** ISO-1 group: Compared with SAP group, pancreatic acinar edema, necrosis, extra-vascular and intra-septal bleeding, and inflammatory cells infiltration are significantly reduced. **e** The histopathological score of the pancreas. Compared with the SO group, $P_a < 0.05$; compared with the SAP group, $P_{ab} < 0.05$; and compared with the ISO-1 group, $P_{bc} < 0.05$

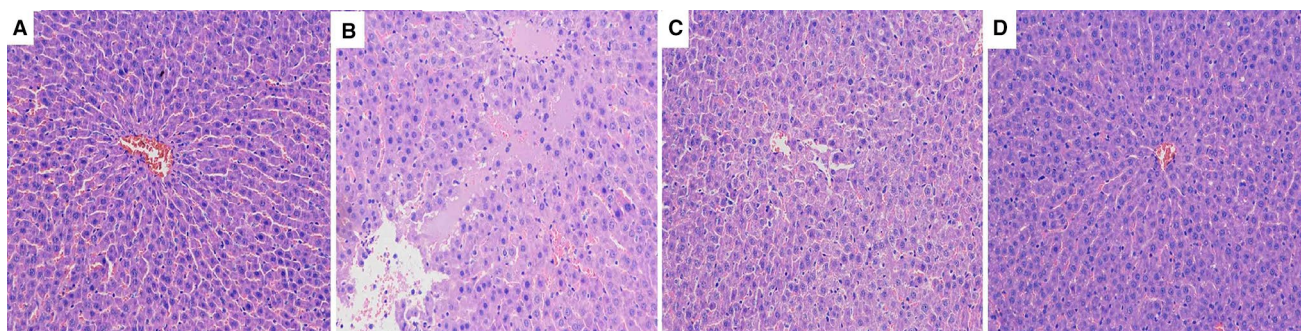


Fig. 2 Pathological changes in rat liver tissue observed by H&E staining (magnification: 400×). **a** and **d** SO and ISO-1 con group: The structure of liver cells is normal, and the arrangement of hepatic cords is orderly. But small partial hepatocytes edema is observed. **b** SAP group. Dot degeneration and necrosis, and large areas of necrosis are observed in liver cells, and the liver cords are partially col-

lapsed. A large number of infiltrated inflammatory cells are observed. **c** ISO-1 group. Point-like degeneration and point-like necrosis are observed in liver cells, and the degree of necrosis is mild, and some liver cords are only slightly disturbed. Pathological injury of liver cells are significantly reduced compared with SAP group

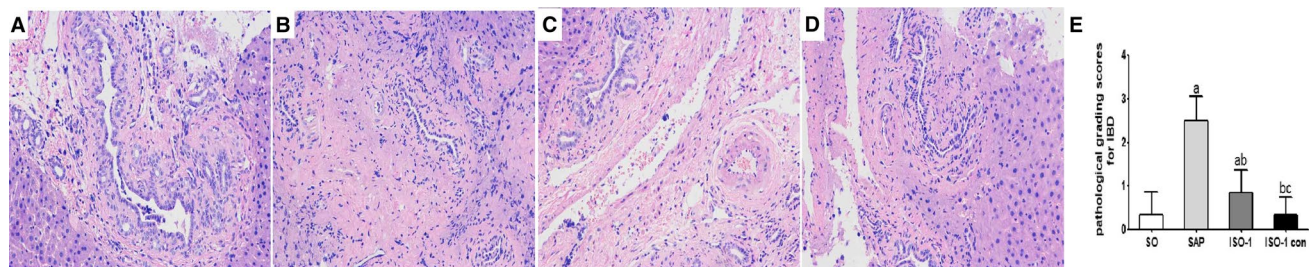


Fig. 3 Pathological changes in the rat IBD cells (magnification: 400×). **a** and **d** SO and ISO-1 con group. The IBD cells show no obvious damage. **b** SAP group. Large areas of IBD cells are necrotic, and substantial inflammatory cell infiltration is observed. **c** ISO-1 group. IBD epithelial cells edema, degeneration, slightly disordered

arrangement and fracture phenomenon, and nuclear deformation are observed. Cells necrosis significantly reduced compared with SAP group. **e** The histopathological score of IBD cells. Compared with the SO group, $P_a < 0.05$; compared with the SAP group, $P_{ab} < 0.05$; and compared with the ISO-1 group, $P_{bc} < 0.05$

Ultrastructural Changes in IBD Cells

According to transmission electron microscopy observations, IBD epithelial cells swelled remarkably in the SAP group, accompanied by many microvilli falling off of the cell surface, mitochondrial vacuolar degeneration, crest disappearance, partial membrane rupture, a glassy matrix, nuclear disappearance, and an expanded endoplasmic reticulum. In the ISO-1 treatment group, all the impairments mentioned above were relieved to some degree. Mitochondria were slightly swollen, part of the mitochondrial matrix was lost, some cristae were fuzzy, but none disappeared, and there was a slight expansion of the rough endoplasmic reticulum. In the SO group and ISO-1 drug control group, we found that the microvilli of IBD epithelial cells were orderly arranged with a clear membrane dual structure, abundant and regular arrangement of mitochondria in the cytoplasm,

slight swelling of a few mitochondria, no obvious swelling of the ridge, no obvious expansion of the rough endoplasmic reticulum, and a basically normal size of the nucleus without deformation (Fig. 4a–d).

Expression of MIF and P38 in IBD Cells

Immunohistochemical S-P analysis revealed that MIF and P38 were widely expressed in IBD cell nuclei in the SAP group, and the labeling signal was strongly positive. Compared with the SAP group, the expression of MIF and P38 in the ISO-1 treatment group was significantly inhibited. The IOD values of MIF and P38 expression were highly significantly different ($P < 0.05$) between the two groups. In contrast, the signals were weak in the SO group and ISO-1 control groups (Figs. 5a–e, 6a–e).

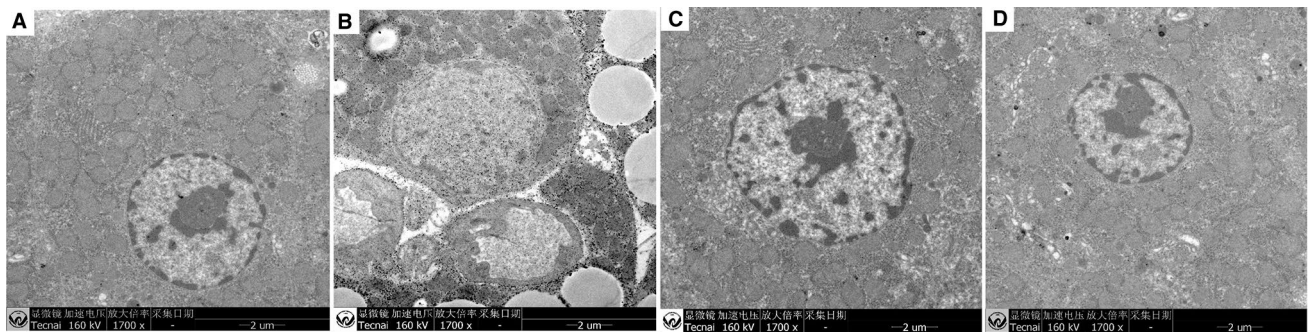


Fig. 4 Ultrastructural changes in rat IBD cells. **a** and **d**. SO and ISO-1 con group. Microvilli in IBD cell is rich, neat, and matrix is uniform, cell crest clearly visible, and the dual structure of the cell membrane distinct. Mitochondria in the cytoplasm is rich, distribution uniform, and arrangement regular. But a small amount of mitochondria mild swelling is observed. Rough endoplasmic reticulum has no obvious expansion, and the nucleus size is normal and no deformation. **b** SAP group. The IBD cells showed obvious edema, and the surface microvilli were sparse, mitochondrial vacuoles dena-

tured, cristae disappeared, and part of the membrane ruptured. The matrix was highly frosted glass, nuclear membrane disappeared, endoplasmic reticulum expanded and unclear. **c** ISO-1 group. The epithelial cells of IBD were partially shed, the cytoplasm was relatively loose, mitochondria slightly swollen and part of the matrix lost, no crest disappeared. The rough endoplasmic reticulum was slightly expanded. The ultrastructural damage was less than that of the SAP group

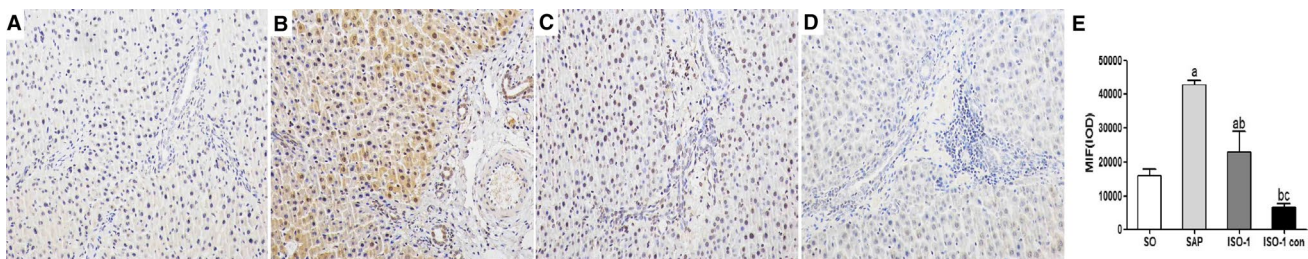


Fig. 5 MIF expression in IBD cells detected by immunohistochemistry. Cells that were positive for MIF expression are dyed tan-yellow. **a** and **d** A small amount of MIF expression was detected in the cytoplasm of IBD cells in the SO group and ISO-1con group. **b** SAP group. The nuclei of IBD in the SAP group were stained brown-yellow, and the MIF protein expression was strongly positive, which was

expressed in the nucleus. **c** ISO-1 group. The expression of MIF protein in the nucleus of IBD was weaker, and its staining was shallower than that in SAP group. **e** Comparison of the IOD values of MIF expression in IBD cells. Compared with the SO group, $P_a < 0.01$; compared with the SAP, $P_{ab} < 0.05$; and compared with the ISO-1 group, $P_{bc} < 0.05$

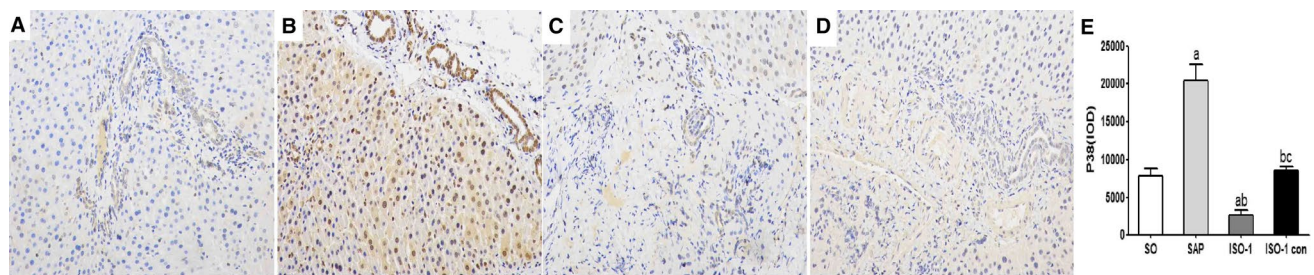


Fig. 6 P38 expression in IBD cells detected by immunohistochemistry. Cells that were positive for P38 expression are dyed tan-yellow. **a** and **d**. A small amount of MIF expression was detected in the cytoplasm of IBD cells in the SO group and ISO-1con group. **b** SAP group. The nucleus of IBD in the SAP group was stained brown-yellow, and the MIF protein expression was strongly positive, which was

expressed in the nucleus. **c** ISO-1 group. The expression of MIF protein in the nucleus of IBD was weaker, and its staining was shallower than that in SAP group. **e** Comparison of the IOD values of MIF expression in IBD cells. Compared with the SO group, $P_a < 0.01$; compared with the SAP, $P_{ab} < 0.05$; and compared with the ISO-1 group, $P_{bc} < 0.05$

MIF mRNA and TNF-mRNA Expression Levels in IBD Cells

The MIF and TNF- α mRNA expression levels in IBD cells significantly increased in the SAP group, as shown by real-time PCR. Both mRNA expression levels determined using the $2^{-\Delta\Delta C_t}$ method were obviously higher in the SAP group than in the SO group and ISO-1 drug control group. The $2^{-\Delta\Delta C_t}$ values of MIF mRNA and TNF- α mRNA expression were highly significantly different ($P < 0.01$) between the SO and SAP groups. Their expression levels in the ISO-1 treatment group were significantly lower than those in the SAP group ($P < 0.05$) (Figs. 7a–e, 8a–f).

NF- κ B p65, P38, p-P38, and TNF- α Protein Expression Levels in IBD Tissues

P38-MAPK expression was activated in IBD cells in the SAP group, and the p-P38 protein expression levels detected by Western blot were obviously higher than those in the SO group and ISO-1 drug control group. However, P38-MAPK expression was suppressed in the ISO-1 treatment group. The results were significantly different ($P < 0.05$) between the ISO-1 treatment group and the SAP group. The NF- κ B p65 and TNF- α protein expression levels changed similar to those of p-P38 (Fig. 9a–e).

Concentrations of TNF- α , IL-1 β , and IL-6 in IBD Tissues

ELISA revealed that the levels of TNF- α , IL-1 β , and IL-6 in IBD cells in the SAP group were markedly higher than those in the SO group and ISO-1 drug control group. Indeed, in this regard, there were highly significant

differences between the SAP group and ISO-1 treatment group ($P < 0.05$) (Fig. 10a–c).

Discussion

ISO-1 ((S,R)-3-(4-hydroxyphenyl)-4,5-dihydro-5-isoxazole acetic acid sandwich ester) is a specific small molecule inhibitor of MIF [6]. It plays a role in prohibiting the binding of MIF to the membrane receptor CD74 but has no side effects on any other inflammatory cells [8]. ISO-1 has promising applicable prospects and has been widely applied in various animal disease models, such as ulcerative colitis, multi-organ dysfunction caused by endotoxaemia, inflammatory diseases, and ischemia–reperfusion injury. Sakai et al. [9] found that the use of anti-MIF antibodies can significantly reduce the mortality rate of SAP rats. Calandra et al. [10] reported that MIF was involved in the pathophysiological process of sepsis and mediated the lethal effects of endotoxin on experimental animals, while the application of anti-MIF could significantly reduce the mortality rate of bacterial peritonitis mice. Other studies showed that the MAPK (P38, ERK1/2, JNK) signaling pathways were activated in an AP mouse model induced by caerulein, and when the mouse was injected intraperitoneally with the high-efficiency ERK kinase (MEK1/2) selective inhibitor PD98059, PD98059 could significantly reverse activation of the MAPK (P38, ERK1/2, JNK) signaling pathways and alleviate pancreatic and liver damage [11].

In many inflammatory disease animal models, such as SAP, once activation of MIF is inhibited by some approach, the development of inflammation and injury to organs can be reversed to some degree, showing promising therapeutic effects of MIF inhibitors on inflammatory diseases [3, 5, 12–14].

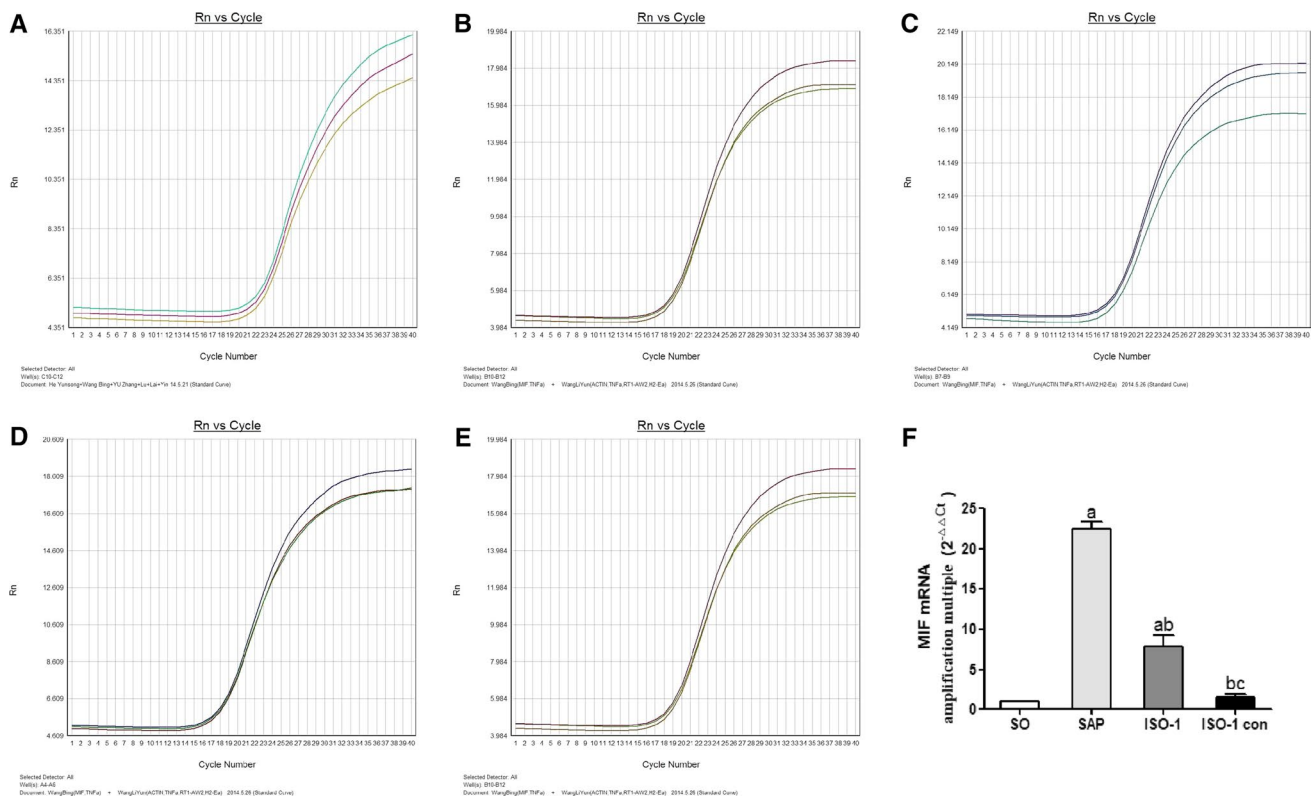


Fig. 7 MIF mRNA expression level in IBD cells of the rats detected by real-time PCR. **a–e** Present maps of the MIF mRNA amplification curve corresponding to actin (internal reference) and the SO, SAP, ISO-1, and ISO-1 con groups, respectively. **f** The MIF mRNA expression level in IBD cells. The value of MIF mRNA expression abun-

dance in IBD cells was significantly higher in SAP group than that in SO and ISO-1 con group. After treated with ISO-1, the expression level decreased obviously. Compared with the SO group, $P_a < 0.01$; compared with the SAP, $P_{ab} < 0.05$; and compared with the ISO-1 group, $P_{bc} < 0.05$

In this research, we focused on exploring the protection of IBD cells by ISO-1 in SAP and its protective effect mechanism using the strong specific MIF inhibitor ISO-1. We found that ISO-1 could notably alleviate the pathological injuries to pancreatic and IBD cells in SAP animal models. After treatment with ISO-1, the pathological damage to pancreatic and IBD cells was significantly alleviated. The degrees of swelling and necrosis of pancreatic acinar and IBD cells were significantly reduced compared with the SAP group, and the pathological score significantly decreased compared with the SAP group. Moreover, there was a significant difference between these groups. Electron microscopy showed that the degree of injury to mitochondria and the rough endoplasmic reticulum in IBD cells was significantly reduced in the ISO-1 group. The results indicated that ISO-1 could help to relieve the degree of inflammatory injuries to IBD cells during SAP and play a protective role on IBD cells in SAP.

Liver macrophages can activate NF- κ B by mediating the P38-MAPK signaling pathway and further induce TNF- α [15, 16]. NF- κ B is a nuclear transcription factor with multidirectional regulation [17]. With the activation

of immune stimulants and other factors, it can bind with the κ B sequence of some gene promoters and enhancers to initiate or enhance the transcription of genes and participate in the regulation of gene transcription and expression related to immune function, inflammatory reactions, and apoptosis [18–21]. Therefore, MIF inhibitors might suppress the inflammatory process by inhibiting the activity of P38-MAPK and further inhibiting the transcriptional functions of NF- κ B. According to the results of our research, ISO-1 could significantly suppress the activation of P38-MAPK in rat IBD cells, downregulate the transcriptional functions of NF- κ B, inhibit the expression of inflammatory factors downstream, and finally play an anti-inflammatory role.

In our study, we found that P38 was expressed in the nucleus of IBD cells, and the positive expression in the ISO-1 treatment group decreased significantly compared with that in the SAP group. Moreover, Western blotting was used to detect the expression levels of the p-p38 protein in IBD cells. The expression level of the p-p38 protein significantly decreased after treatment with ISO-1. Similarly, the expression level of NF- κ B P65 in IBD cells

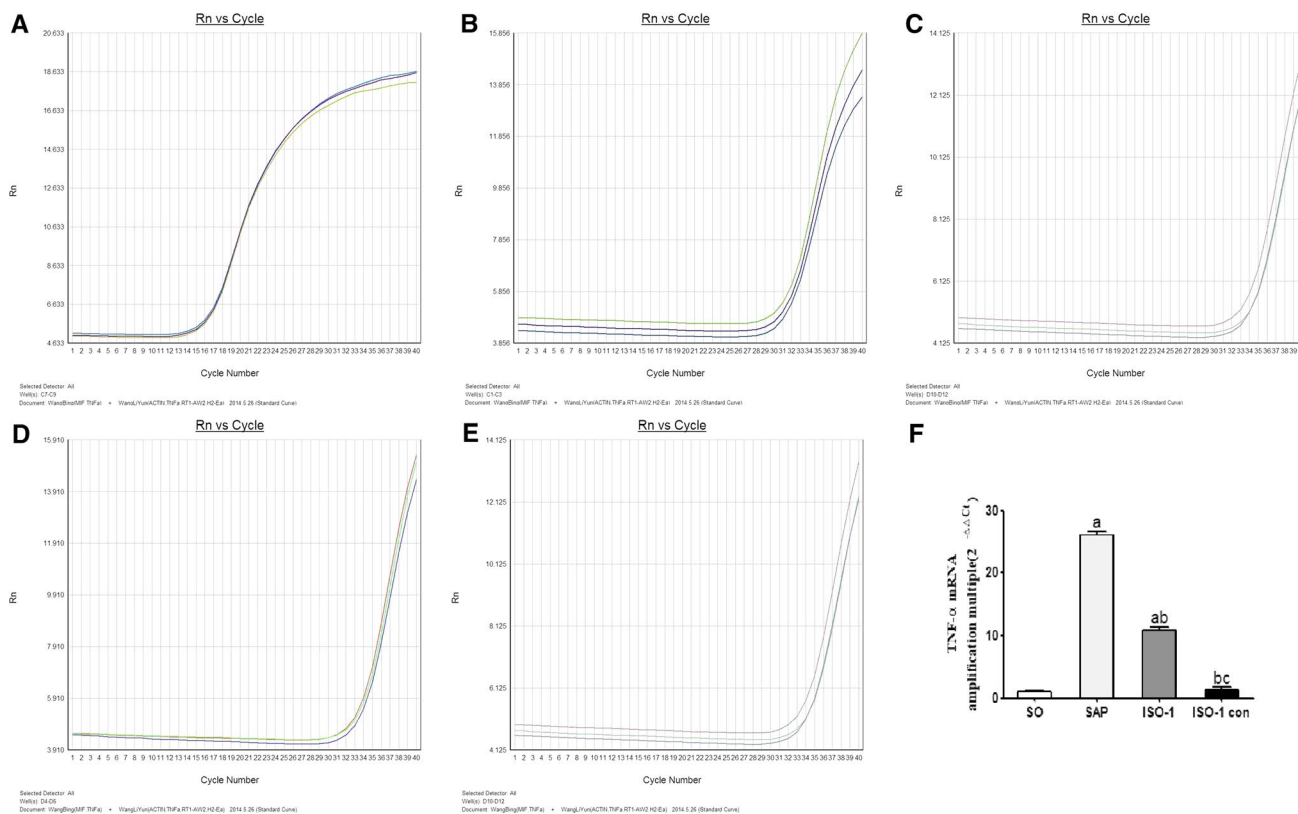
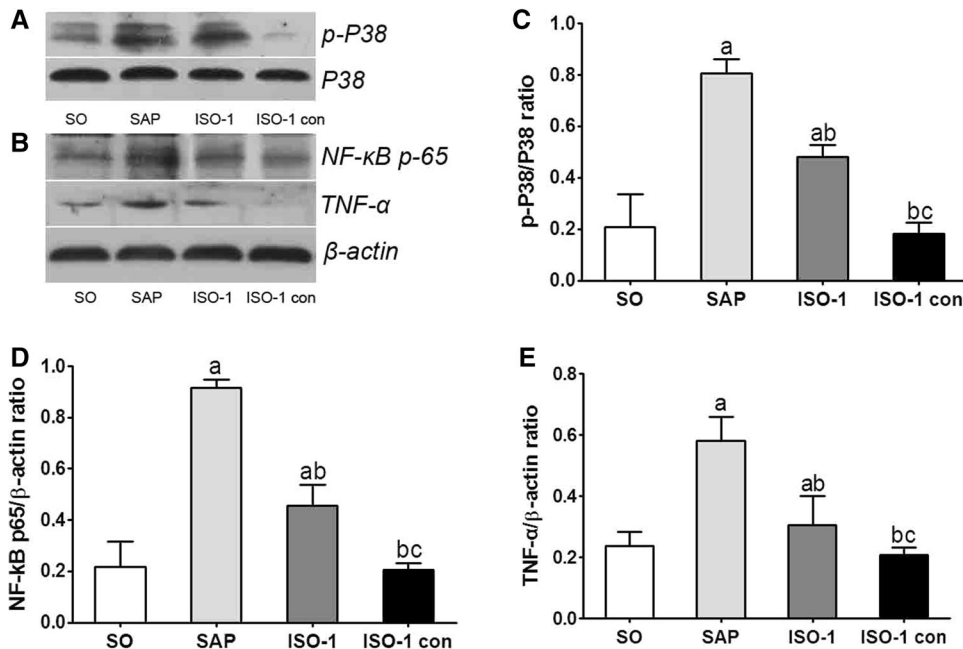


Fig. 8 TNF-α mRNA expression level in the IBD cells of rats detected by real-time PCR. **a–e** Present maps of the TNF-a mRNA amplification curve corresponding to actin (internal reference) and the SO, SAP-3 h, SAP-6 h, and SAP-12 h groups, respectively. **f** The TNF-α mRNA expression level. The value of TNF-α mRNA expres-

sion abundance in IBD cells was significantly higher in SAP group than that in SO and ISO-1 con group. After treated with ISO-1, the expression level decreased obviously. Compared with the SO group, Pa < 0.01; compared with the SAP, Pab < 0.05; and compared with the ISO-1 group, Pbc < 0.05

Fig. 9 Protein expression levels of P38, P-P38, NF-κB p65, and TNF-α in the IBD cells of rats as measured by Western blot. **a** and **b** P38, P-P38, NF-κB p65, and TNF-α protein electrophoresis banding. **c–e** Present the analysis of the protein expression OD values for P-P38, NF-κB p65, and TNF-α, respectively. Compared with the SO group, Pa < 0.05; compared with the SAP group, Pab < 0.05; and compared with the ISO-1 group, Pbc < 0.05



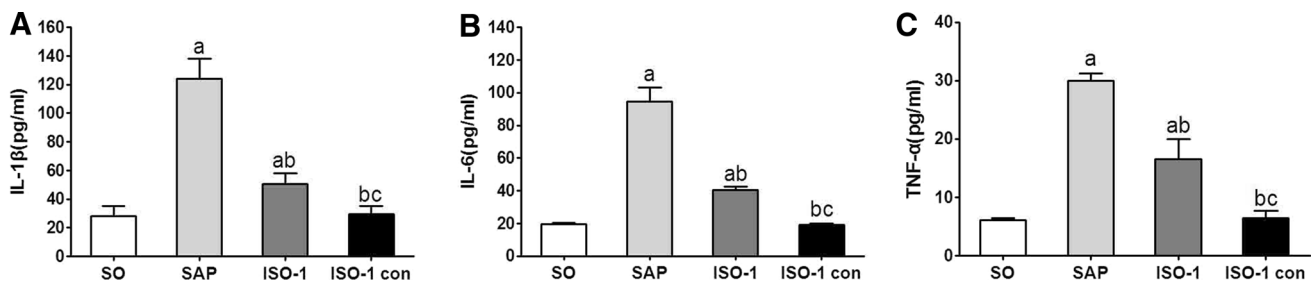


Fig. 10 Contents of IL-1 β , IL-6 and TNF- α in the IBD cells of rats as measured by ELISA. **a–c.** present the results of the comparative analysis of the contents of IL-1 β , IL-6, and TNF- α , respectively. Com-

pared with the SO group, $P_a < 0.05$; compared with the SAP group, $P_{ab} < 0.05$; and compared with the ISO-1 group, $P_{bc} < 0.05$

was significantly decreased in the ISO-1 treatment group compared with the SAP group. This difference was statistically significant.

In the pathogenesis of acute pancreatitis, TNF- α is also a key inflammatory mediator [22], and its overexpression can induce the expression of inflammation-related genes and cause cell death, endothelial cell dysfunction, and the recruitment of activated inflammatory cells [23, 24]. In addition, studies have found that IL-6 is the main factor that stimulates the synthesis of the acute protein response during the pathogenesis of SAP, and the sustained release of IL-6 during SAP leads to the uncontrolled expression of other important anti-inflammatory transmitters or cytokine inhibitors [25]. Studies have confirmed that IL-6 is closely associated with SIRS and MODS, and serum IL-6 levels are positively correlated with the severity of acute pancreatitis.

In addition, some researchers have found that activation of IL-1 β is involved in the development of pancreatic injury and the inflammatory response by applying an acute pancreatitis mouse model with IL-1 β receptor knockout [26].

In this study, ELISA showed that the expression levels of the inflammatory factors TNF- α , IL-6, and IL-1 β in IBD tissues treated with ISO-1 were significantly lower than those in the SAP group. Therefore, we think that ISO-1 could effectively suppress the expression levels of TNF- α , IL-1 β , and IL-6 in IBD cells and relieve inflammatory responses in SAP.

In summary, our study inferred that the MIF-specific inhibitor ISO-1 could effectively block the expression of MIF in IBD cells, suppress the activation of the P38-MAPK signaling pathway, reduce the activity of NF- κ B, and down-regulate the expression of inflammatory cytokines such as TNF- α , IL-1 β and IL-6. As a result, neutrophil infiltration mediated by NF- κ B could be blocked, and pathological damage to the pancreas and IBD tissue and ultrastructural changes could be partially reversed. Therefore, the inflammatory injuries to IBD cells during the SAP process were relieved. All the results suggest a MIF as promising therapeutic target for SAP by focusing on MIF-specific inhibitors.

However, more research on inflammatory factors during SAP is urgently needed, and we look forward to the discovery and application of highly specific MIF inhibitors. In addition, transgenic animals will provide us with a deeper understanding of SAP and its associated IBD cellular injuries, helping us to further explore and improve the clinical treatment of SAP.

Compliance with Ethical Standards

Conflict of interest This study has no conflict of interest with any organization or individual.

References

1. Wang B, Zhao KL, Hu WJ, Zuo T, Ding YM, Wang WX. Macrophage migration inhibitor promoted the intrahepatic bile duct injury in rats with severe acute pancreatitis. *Dig Dis Sci.* 2019;64:759–772. <https://doi.org/10.1007/s10620-018-5379-7>.
2. Aeberli D, Yang Y, Mansell A, et al. Endogenous macrophage migration inhibitory factor modulates glucocorticoid sensitivity in macrophages via effects on MAP kinase phosphatase-1 and p38 MAP kinase. *FEBS Lett.* 2006;580:974–981.
3. Chuang CC, Chuang YC, Chang WT, et al. Macrophage migration inhibitory factor regulates interleukin-6 production by facilitating nuclear factor- κ B activation during *Vibrio vulnificus* infection. *BMC Immunol.* 2010;11:50.
4. Takahashi K, Koga K, Linge HM, et al. Macrophage CD74 contributes to MIF-induced pulmonary inflammation. *Respir Res.* 2009;10:33.
5. Paszt A, Eder K, Szabolcs A, et al. Effects of glucocorticoid agonist and antagonist on the pathogenesis of L-arginine-induced acute pancreatitis in rat. *Pancreas.* 2008;36:369–376.
6. Schmidt J, Rattner DW, Lewandrowski K, et al. A better model of acute pancreatitis for evaluating therapy. *Ann Surg.* 1992;215:44–56.
7. Suzuki S, Toledo-Pereyra LH, Rodriguez FJ, et al. Neutrophil infiltration as an important factor in liver ischemia and reperfusion injury. Modulating effects of FK506 and cyclosporine. *Transplantation.* 1993;5:265–1272.
8. Lubetsky JB, Dios A, Han J, et al. The tautomerase active site of macrophage migration inhibitory factor is a potential target

- for discovery of novel anti-inflammatory agents. *J Biol Chem*. 2002;277:24976–24982.
9. Sakai Y, Masamune A, Satoh A, et al. Macrophage migration inhibitory factor is a critical mediator of severe acute pancreatitis. *Gastroenterology*. 2003;124:725–736.
 10. Calandra T, Roger T. Macrophage migration inhibitory factor: a regulator of innate immunity. *Nat Rev Immunol*. 2003;3:791–800.
 11. Mazzon E, Impellizzeri D, Di Paola R, et al. Effects of mitogen-activated protein kinase signaling pathway inhibition on the development of cerulein-induced acute pancreatitis in mice. *Pancreas*. 2012;41:560–570.
 12. Nattee P, Honsawek S, Chongsrisawat V, et al. Elevated serum macrophage migration inhibitory factor levels in post-operative biliary atresia. *Asian J Surg*. 2009;32:109–113.
 13. Nakajima H, Takagi H, Horiguchi N, et al. Lack of macrophage migration inhibitory factor protects mice against concanavalin A-induced liver injury. *Liver Int*. 2006;26:346–351.
 14. Chuang CC, Wang ST, Chen WC, et al. Increases in serum macrophage migration inhibitory factor in patients with severe sepsis predict early mortality. *Shock*. 2007;27:503–506.
 15. Murr MM, Yang J, Fier A, et al. Regulation of Kupffer cell TNF gene expression during experimental acute pancreatitis: the role of p38-MAPK, ERK1/2, SAPK/JNK, and NF- κ B. *J Gastrointest Surg*. 2003;7:20–25.
 16. Murr MM, Yang J, Fier A, et al. Pancreatic elastase induces liver injury by activating cytokine production within Kupffer cells via nuclear factor- κ B. *J Gastrointest Surg*. 2002;6:474–480.
 17. Hietaranta A, Mustonen H, Puolakkainen P, et al. Proinflammatory effects of pancreatic elastase are mediated through TLR4 and NF- κ B. *Biochem Biophys Res Commun*. 2004;323:192–196.
 18. Cuzzocrea S, Mazzon E, Di Paola R, et al. Glycogen synthase kinase-3 beta inhibition attenuates the degree of arthritis caused by type II collagen in the mouse. *Clin Immunol*. 2006;120:57–67.
 19. Yu J, Deng WH, Wang WX, et al. Inhibition of poly(ADP-ribose) polymerase attenuates acute kidney injury in sodium taurocholate-induced acute pancreatitis in rats. *Pancreas*. 2012;41:1299–1305.
 20. Deng H, Zhang N, Wang Y, et al. S632A3, a new glutarimide antibiotic, suppresses lipopolysaccharide-induced pro-inflammatory responses via inhibiting the activation of glycogen synthase kinase 3 beta. *Exp Cell Res*. 2012;318:2592–2603.
 21. Deng WH, Yu J, Wang WX, et al. Zerumbone attenuates the severity of acute necrotizing pancreatitis and pancreatitis-induced hepatic injury. *Mediators Inflamm*. 2012;2012: 156507.
 22. Schafer C, Tietz AB, Goke B. Pathophysiology of acute experimental pancreatitis: lessons from genetically engineered animal models and new molecular approaches. *Digestion*. 2005;71:162–172.
 23. Granger J, Remick D. Acute pancreatitis: models, markers, and mediators. *Shock*. 2005;24:45–51.
 24. Pastor CM, Frossard JL. Are genetically modified mice useful for the understanding of acute pancreatitis. *FASEB J*. 2001;15:893–897.
 25. Gulcubuk A, Altunatmaz K, Sonmez K, et al. Effects of curcumin on tumour necrosis factor-alpha and interleukin-6 in the late phase of experimental acute pancreatitis. *J Vet Med A Physiol Pathol Clin Med*. 2006;53:49–54.
 26. Abcouwer S F, Norman J, Fink G, et al. Tissue-specific regulation of glutamine synthetase gene expression in acute pancreatitis is confirmed by using interleukin-1 receptor knockout mice. *Surgery*. 1996, 120: 255–263, 263–264.

Publisher's Note Springer Nature remains neutral with regard to jurisdictional claims in published maps and institutional affiliations.